AD_____

GRANT NO: DAMD17-94-J-4367

TITLE: Development of an Inverse Technique to Estimate the Ultrasound Field During Chest Wall and Breast Hyperthermia

PRINCIPAL INVESTIGATOR(S): Andrew W. Dutton, Ph.D.

CONTRACTING ORGANIZATION: University of Utah
Salt Lake City, Utah 84112

REPORT DATE: August 28, 1995

TYPE OF REPORT: Annual

PREPARED FOR: U.S. Army Medical Research and Materiel Command
Fort Detrick, Maryland 21702-5012

DISTRIBUTION STATEMENT: Approved for public release;
distribution unlimited

REPORT DOCUMENTATION PAGE

Form Approved
OMB No. 0704-0188

1. AGENCY USE ONLY (Leave blank)	2. REPORT DATE	3. REPORT TYPE AND DATES COVERED
	28 Aug 95	Annual 1 Aug 94 - 31 Jul 95

4. TITLE AND SUBTITLE
Development of an Inverse Technique to Estimate the Ultrasound Field During Chest Wall and Breast Hyperthermia

5. FUNDING NUMBERS
DAMD17-94-J-4367

6. AUTHOR(S)
Andrew W. Dutton, Ph.D.

7. PERFORMING ORGANIZATION NAME(S) AND ADDRESS(ES)
University of Utah
Salt Lake City, Utah 84112

8. PERFORMING ORGANIZATION REPORT NUMBER

9. SPONSORING / MONITORING AGENCY NAME(S) AND ADDRESS(ES)
U.S. Army Medical Research and Materiel Command
Fort Detrick, Maryland 21702-5012

10. SPONSORING / MONITORING AGENCY REPORT NUMBER

11. SUPPLEMENTARY NOTES

12a. DISTRIBUTION / AVAILABILITY STATEMENT
Approved for public release; distribution unlimited

12b. DISTRIBUTION CODE

13. ABSTRACT *(Maximum 200 words)*

A clinical system is being constructed to use inverse techniques to estimate the absorbed power field in the breast and chest wall during ultrasound hyperthermia. The system uses a B-mode ultrasound imager to construct a geometric model based upon each patient's anatomy and to initially measure the ultrasound attenuation coefficient at selected areas within the tissue region. The goal is to provide a tool to accurately estimate the ultrasound field so as to ensure therapeutic heating of the tumor while minimizing patient pain. In the first year of this project, all the clinical ultrasound data acquisition equipment has been built and integrated. Advanced two-dimensional numerical models of the ultrasound field using finite elements and integral equation methods have been developed. Future work will include numerical model verification studies, modification of the clinical thermocouple probes to measure the absorbed power and integration of all the components into the inverse technique.

14. SUBJECT TERMS
Breast Cancer, Hyperthermia, Ultrasound, Inverse Theory

15. NUMBER OF PAGES
28

16. PRICE CODE

17. SECURITY CLASSIFICATION OF REPORT	18. SECURITY CLASSIFICATION OF THIS PAGE	19. SECURITY CLASSIFICATION OF ABSTRACT	20. LIMITATION OF ABSTRACT
Unclassified	Unclassified	Unclassified	Unlimited

GENERAL INSTRUCTIONS FOR COMPLETING SF 298

The Report Documentation Page (RDP) is used in announcing and cataloging reports. It is important that this information be consistent with the rest of the report, particularly the cover and title page. Instructions for filling in each block of the form follow. It is important to *stay within the lines* to meet *optical scanning requirements*.

Block 1. Agency Use Only *(Leave blank)*.

Block 2. Report Date. Full publication date including day, month, and year, if available (e.g. 1 Jan 88). Must cite at least the year.

Block 3. Type of Report and Dates Covered. State whether report is interim, final, etc. If applicable, enter inclusive report dates (e.g. 10 Jun 87 - 30 Jun 88).

Block 4. Title and Subtitle. A title is taken from the part of the report that provides the most meaningful and complete information. When a report is prepared in more than one volume, repeat the primary title, add volume number, and include subtitle for the specific volume. On classified documents enter the title classification in parentheses.

Block 5. Funding Numbers. To include contract and grant numbers; may include program element number(s), project number(s), task number(s), and work unit number(s). Use the following labels:

C	- Contract	PR	- Project
G	- Grant	TA	- Task
PE	- Program Element	WU	- Work Unit Accession No.

Block 6. Author(s). Name(s) of person(s) responsible for writing the report, performing the research, or credited with the content of the report. If editor or compiler, this should follow the name(s).

Block 7. Performing Organization Name(s) and Address(es). Self-explanatory.

Block 8. Performing Organization Report Number. Enter the unique alphanumeric report number(s) assigned by the organization performing the report.

Block 9. Sponsoring/Monitoring Agency Name(s) and Address(es). Self-explanatory.

Block 10. Sponsoring/Monitoring Agency Report Number. *(If known)*

Block 11. Supplementary Notes. Enter information not included elsewhere such as: Prepared in cooperation with...; Trans. of...; To be published in.... When a report is revised, include a statement whether the new report supersedes or supplements the older report.

Block 12a. Distribution/Availability Statement. Denotes public availability or limitations. Cite any availability to the public. Enter additional limitations or special markings in all capitals (e.g. NOFORN, REL, ITAR).

DOD - See DoDD 5230.24, "Distribution Statements on Technical Documents."
DOE - See authorities.
NASA - See Handbook NHB 2200.2.
NTIS - Leave blank.

Block 12b. Distribution Code.

DOD - Leave blank.
DOE - Enter DOE distribution categories from the Standard Distribution for Unclassified Scientific and Technical Reports.
NASA - Leave blank.
NTIS - Leave blank.

Block 13. Abstract. Include a brief *(Maximum 200 words)* factual summary of the most significant information contained in the report.

Block 14. Subject Terms. Keywords or phrases identifying major subjects in the report.

Block 15. Number of Pages. Enter the total number of pages.

Block 16. Price Code. Enter appropriate price code *(NTIS only)*.

Blocks 17. - 19. Security Classifications. Self-explanatory. Enter U.S. Security Classification in accordance with U.S. Security Regulations (i.e., UNCLASSIFIED). If form contains classified information, stamp classification on the top and bottom of the page.

Block 20. Limitation of Abstract. This block must be completed to assign a limitation to the abstract. Enter either UL (unlimited) or SAR (same as report). An entry in this block is necessary if the abstract is to be limited. If blank, the abstract is assumed to be unlimited.

FOREWORD

Opinions, interpretations, conclusions and recommendations are those of the author and are not necessarily endorsed by the US Army.

AO Where copyrighted material is quoted, permission has been obtained to use such material.

AO Where material from documents designated for limited distribution is quoted, permission has been obtained to use the material.

AO Citations of commercial organizations and trade names in this report do not constitute an official Department of Army endorsement or approval of the products or services of these organizations.

AO In conducting research using animals, the investigator(s) adhered to the "Guide for the Care and Use of Laboratory Animals," prepared by the Committee on Care and Use of Laboratory Animals of the Institute of Laboratory Resources, National Research Council (NIH Publication No. 86-23, Revised 1985).

AO For the protection of human subjects, the investigator(s) adhered to policies of applicable Federal Law 45 CFR 46.

AO In conducting research utilizing recombinant DNA technology, the investigator(s) adhered to current guidelines promulgated by the National Institutes of Health.

AO In the conduct of research utilizing recombinant DNA, the investigator(s) adhered to the NIH Guidelines for Research Involving Recombinant DNA Molecules.

AO In the conduct of research involving hazardous organisms, the investigator(s) adhered to the CDC-NIH Guide for Biosafety in Microbiological and Biomedical Laboratories.

Accesion For	
NTIS CRA&I	☒
DTIC TAB	☐
Unannounced	☐
Justification	
By	
Distribution /	
Availability Codes	
Dist	Avail and / or Special
A-1	

Andrew W Pittman
PI - Signature Date

Contents

Nomenclature

$\tilde{A}$	complex pressure amplitude
c	wave speed
e	error
f	cyclical frequency
I	pressure intensity
k	wave number
p	total pressure
p_o	ambient pressure
p'	acoustic pressure
$\hat{p}$	complex pressure
q_v	internal thermal energy generation
Q	measured quantity
J	jacobian
r	linear position coordinate
s	surface of the transducer
t	time
$\mathbf{u}$	total velocity
$\mathbf{u}_o$	ambient velocity
$\mathbf{u}'$	acoustic velocity
v_s	surface velocity of radiator
α	pressure attenuation coefficient
β	pressure attenuation slope coefficient
γ	model parameter
ρ	total density
ρ_o	ambient density
ρ'	acoustic density
$\mathbf{x}$	position
Z	acoustic impedance
κ_s	compressibility (inverse of bulk modulus)
μ	absorption coefficient
π	pi
Φ	cost function
Ψ	velocity potential
ω	radial frequency

1 Introduction

Hyperthermia has been shown to be an efficacious adjuvant therapy in the treatment of recurrent breast cancer [1, 2] and recent clinical trials continue to demonstrate the benefit of adjuvant hyperthermia in the radiotherapy treatment of recurrent breast cancer [3]. These positive results have been realized through a variety of clinical hyperthermia heating devices, including radiative electromagnetic applicators [4, 5] and ultrasound based devices [6]. Moreover, these positive results have been realized in spite of the fact that the clinically achieved thermal doses were below those though to provide direct thermal cytotoxicity and thermal radio-sensitization [7, 8]. These low thermal doses are attributed to two factors [9]: 1) patient pain that limits the treatment, and 2) technical limitations in the ability of the device to raise the tumor temperature to the therapeutic level. The work in this research directly addresses the second issue of technical limitation and indirectly addresses the issue of patient pain.

1.1 Goals

A clinical system is being constructed to use inverse techniques to estimate the absorbed power field in the breast and chest wall during ultrasound hyperthermia. The system uses a B-mode ultrasound imager to construct a geometric model based upon each patient's anatomy and to initially measure the ultrasound attenuation coefficient at selected areas within the tissue region. Ultrasound propagation from the transducer and into the breast is modeled with a hybrid of Green's function solutions used in the homogenous water region and a finite element solution of the acoustic wave equation in the inhomogeneous breast region. During the treatment, actual absorbed power will be measured at the thermocouple junctions within the tumor and normal tissue. These absorbed powers will be compared to the modeled absorbed powers at those locations and the ultrasound model will be updated to bring its estimate, which is of the entire ultrasound field, in line with the measured absorbed powers. This updating constitutes the "inverse problem."

It is the goal of this research to provide improved numerical modeling of ultrasound propagation through breast tissue and the post-mastectomy chest wall for use in patient treatment planning of hyperthermia cancer treatments. The clinical hyperthermia situation is diagramed in figure 1. With this improved model the clinician can plan an ultrasound hyperthermia treatment so as to produce the required thermal dose while minimizing patient pain due to excessive temperature or ultrasound-tissue interactions. This improved planning will aid the clinicians in providing better hyperthermia treatments which will improve treatment response rates. This will be done by:

1. developing a clinical data acquisition system to obtain patient anatomy, measure attenuation, and measure absorbed power
2. developing improved models of ultrasound propagation through breast tissue
3. integrating the measurement and modeling techniques into an inverse solution to obtain the "best" solution possible

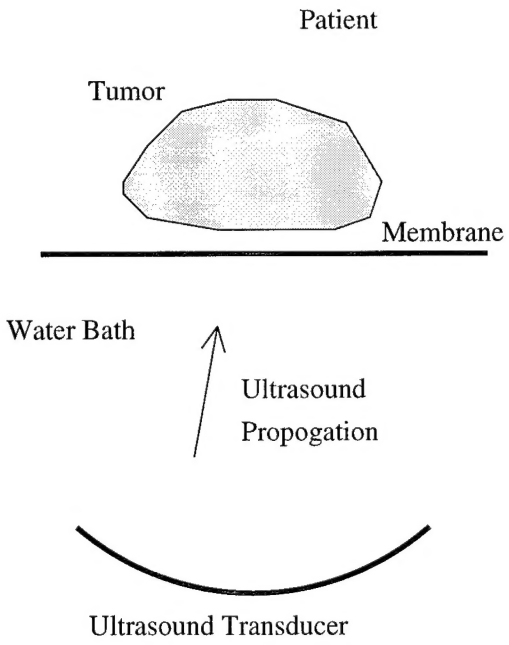

Figure 1: Diagram of the clinical situation for a hyperthermia treatment of the breast or chest wall area.

4. determining the sensitivity of outcomes to input parameters

5. quantifying errors within the measurement and modeling techniques

2 Experimental Methods

All inverse techniques are based upon comparing the results of theoretical models to actual experimental values. The model is updated so that its predictions match the measurements. The experimental platform is therefore an essential and key component of any inverse technique. The advantage of the inverse technique is that the model can predict the pressure field everywhere, while the measurements may be severely restricted, especially in a medical application.

2.1 Data Acquisition

Since this research is designed to be used in conjunction with a clinical system, all data acquisition must be compatible with the current hyperthermia system. Due to physical constraints imposed by the unit and the tumor treatment sites, this requirement limits data acquisition to B-mode ultrasound images and an existing thermocouple based thermometry system. There are therefore two separate data acquisition systems available for the development of the proposed inverse technique. The first is an ultrasound imager used to obtain patient geometry and measure attenuation. The second is the thermocouple thermometry system which can be used to measure the absorbed power.

2.1.1 Geometric Model Construction

Figure 2 diagrams the ultrasound based data acquisition system which consists of a B-mode ultrasound imager[1] to acquire patient geometry. This image will serve as the diagnostic medical image that the geometric model will be based upon.

The construction of the geometric model is the most labor intensive step in solving for the propagation of ultrasound through tissue. In this step, it is necessary to determine the exterior boundary, the boundary conditions, and the internal spatial distribution of material properties and enter these data into the computer for analysis. The most common technique in use today is to base the geometric model upon a standard diagnostic medical image such as CT or MRI [10]. Regions of interest are then traced out over this image and the interior region is meshed for the appropriate numerical solution.

In the first stage of this work only two-dimensional models will be constructed based upon a single image from the B-mode scanner. The imager is equipped with a software measurement package and a hard copy output device. The operator will capture the image of interest, determine regions of constant material properties, measure the dimensions of these regions, and print-out that image.

Once the geometric information is obtained, a two dimensional unstructured mesh generator [2] is used to mesh the domain with quadrilateral elements for a finite element analysis explained in section 3.

[1] Scanner 250, Pie Medical USA 3535 Route 66, Neptune NJ 07753

[2] The program FASTQ was obtained in the ACCESS package from Sandia National Laboratories, Albuquerque, New Mexico 857185-0441, attn: Organization 1503

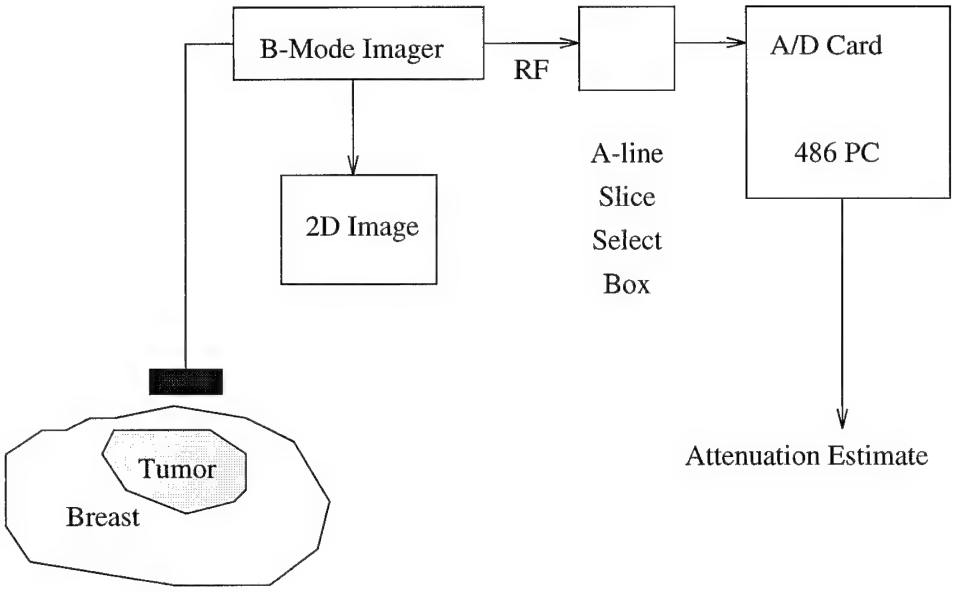

Figure 2: Diagram of the B-mode ultrasound imager based clinical data acquisition system used to obtain patient geometry and measure attenuation for input into the inverse technique.

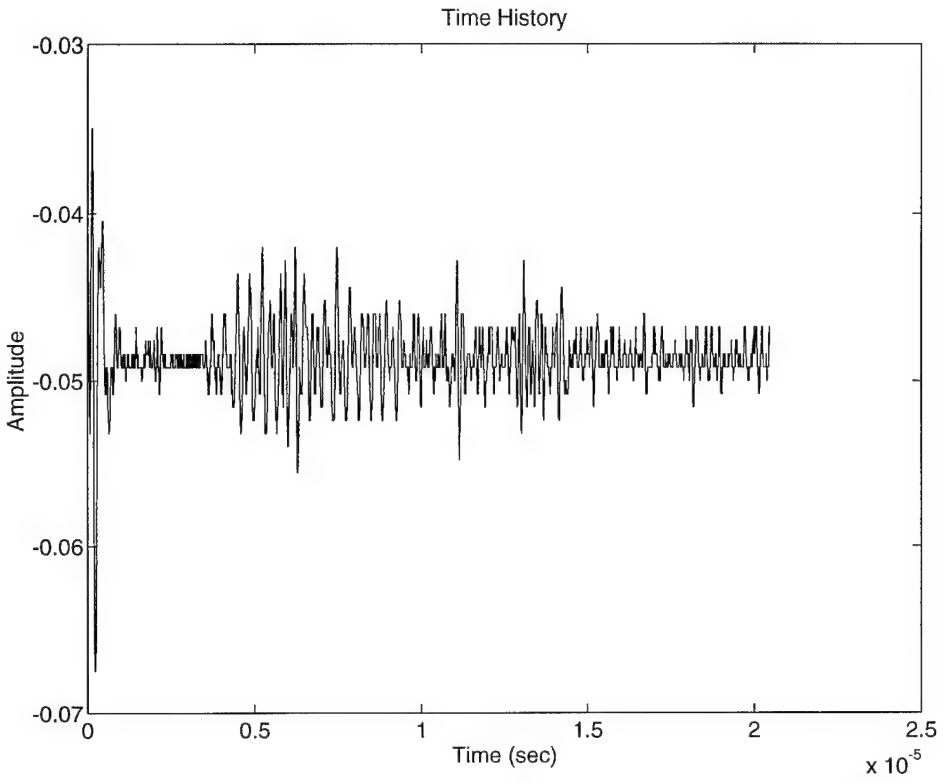

Figure 3: A single line of RF data obtained from the commercial B-mode imager.

2.1.2 A-line Acquisition

Previous researchers have reported on attenuation measurements with clinical ultrasound units [11, 12, 13, 14]. The attenuation measurements were usually used to assist in differential diagnosis of disease, for example breast cancer [15, 16], liver disease [17, 18], or degenerative plaque [19].

For this research the manufacturer has modified the B-mode imager to provide access to the radio-frequency signal from each A-line of the B-mode image. A specific A-line can be selected through a computer controlled *A-line selection circuit* [3]. The radio frequency (RF) data from that A-line is then digitized [4] and stored in a 486 PC. Figure 3 shows an example of a single A-line of RF data. These data are used to measure the tissue attenuation coefficient as explained in section 2.2.1.

[3] Custom circuit manufactured by Mike Jolley at the University of Utah

[4] Gage Applied Sciences Inc., Compuscope 250

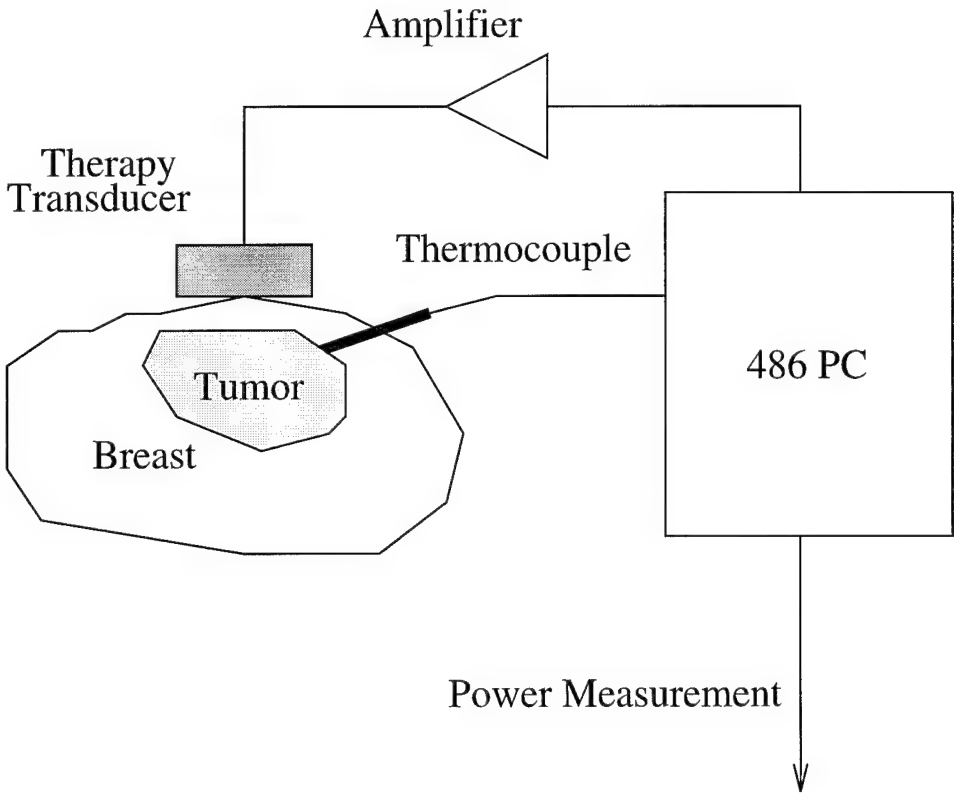

Figure 4: Diagram of the clinical data acquisition system used to obtain on-line measurements of the absorbed power at the thermocouple locations.

2.1.3 Temperature Acquisition

Figure 4 diagrams the clinical treatment data acquisition system in place at the University of Utah's Department of Radiology, Division of Radiation Therapy to measure the tissue temperature from thermocouple probes. It consists of therapeutic ultrasound transducers for heating the tumor and invasive thermocouple probes that are measured through a 486 PC. This system will be used to obtain the time temperature histories needed to measure absorbed power as explained in section 2.2.2.

2.2 Data Analysis

2.2.1 Attenuation Estimation

As an acoustic pressure wave propagates through a medium it loses a portion of its energy through the effects of absorption, reflection, and scattering. The cumulative effect of these phenomenon is referred to as attenuation. Detailed discussion of these phenomenon are discussed in [20, 21]. In practice only the attenuation coefficient, α, is usually sought and its influence upon the amplitude of the pressure distribution is given by

$$|\hat{p}| = |\hat{p}|_{x=0} e^{-\alpha x} \tag{1}$$

A note needs to be made here regarding the definition of attenuation. The attenuation , α, as defined by equation 1 may be more precisely termed the pressure amplitude attenuation coefficient, α_p. This is how attenuation is classically defined in textbooks [21, 22] and how it is used in appendix A. In the majority of studies referenced herein, however, attenuation has been defined as the intensity amplitude attenuation factor, α_i [23]

$$I = I_o e^{\alpha_i x} \tag{2}$$

Since the intesity is proportional to the square of the pressure amplitude, the two definitions are related by

$$2\alpha_p = \alpha_i \tag{3}$$

This distinction is rarely drawn in the literature and in none of the work cited herein. It is important to keep the distinction correct when using values from the literature to calculate pressure fields. Additionally α is usually assumed to be linear function of frequency such that

$$\alpha = \beta \times f \tag{4}$$

As was demonstrated in the original proposal the relative importance of the various acoustic material properties in determining the absorbed power field in the tissue are: the attenuation coefficient ($O(10^{10})$), the tissue speed of sound ($O(10^7)$), and the tissue acoustical impedance ($O(1)$). It is therefore of great importance to obtain accurate attenuation estimates.

Work on *in vivo* measurement of tissue attenuation using echo information has been reviewed in the literature [23]. focused on the liver [12, 24]. These studies show a large spread in attenuation coefficients between patients with values ranging from 0.214 to 0.849 dB/cm/MHz. This relatively large variablity amongst tissues highlights the need for individual measurements for each patient, even on each treatment day. Several methods have been proposed for measuring the attenuation from echo data with some methods accurate to within 1% in phantom studies [11]. They can be categorized as time domain and frequency domain methods.

Frequency Domain Methods The frequency domain methods utilize the fact that the energy in a wave is dissipated as it travels through a length of tissue, see equation 2, and measure the attenuation coefficient by means of the log spectral difference [25, 26, 17, 27, 15, 28, 29, 30, 31], or the shift in the center frequency of the sound pulse [14, 12, 32, 33, 34]. Other methods measure the decay rate with depth of the magnitude of the backscattered pressure at a discete frequency [18, 35, 36]. Still others have developed novel unique methods [37, 38]. Figure 5 shows the power spectral density for the A-line shown in figure 3.

Time Domain Methods Time domain methods are not as popular as the frequency domain methods. They can be based upon measureing the amplitude loss of the signal [13] or novel techniques such as the difference ratio correction method [39].

Finally, Halpren [11] compared five of the above methods for estimating tissue attenuation using a 3.5 MHz Ultramark-9 unit. He reported that,"...a combination of frequency and time domain methods was likely to provide more reliable estimates of attenuation ...."

2.2.2 Acoustic Pressure Measurement

There are currently four accepted methods [40] to measure the acoustic pressure field from an ultrasound transducer:

Hydrophone Places a PVDF needle-like hydrophone in the CW field and measures absolute complex pressures

Radiation Force The transducer sonicates an absorbing target and the resulting force is proportional to the total power

Thermal Techniques Places a thermocouple probe embedded in an absorbing medium in the pulsed field and measures the magnitude of the pressure squared

Optical Techniques Measures the ultrasonic density variation through diffraction techniques to measure the power along a line

Since this research is based upon developing a clinical method utilizing the existing thermocouple information in a clinical hyperthermia situation, only thermal techniques can be utilized. Details of the original technique can be found in [41, 42] with more recent applications discussed in [43, 44, 45, 46]. The relation between the absorbed power due to relaxation (as measured by the thermal techniques) and the acoustic pressure as calculated by the numerical models was put forth by Nyborg [47] as

$$< q_v >= \mu \frac{p_o^2}{\rho c} \tag{5}$$

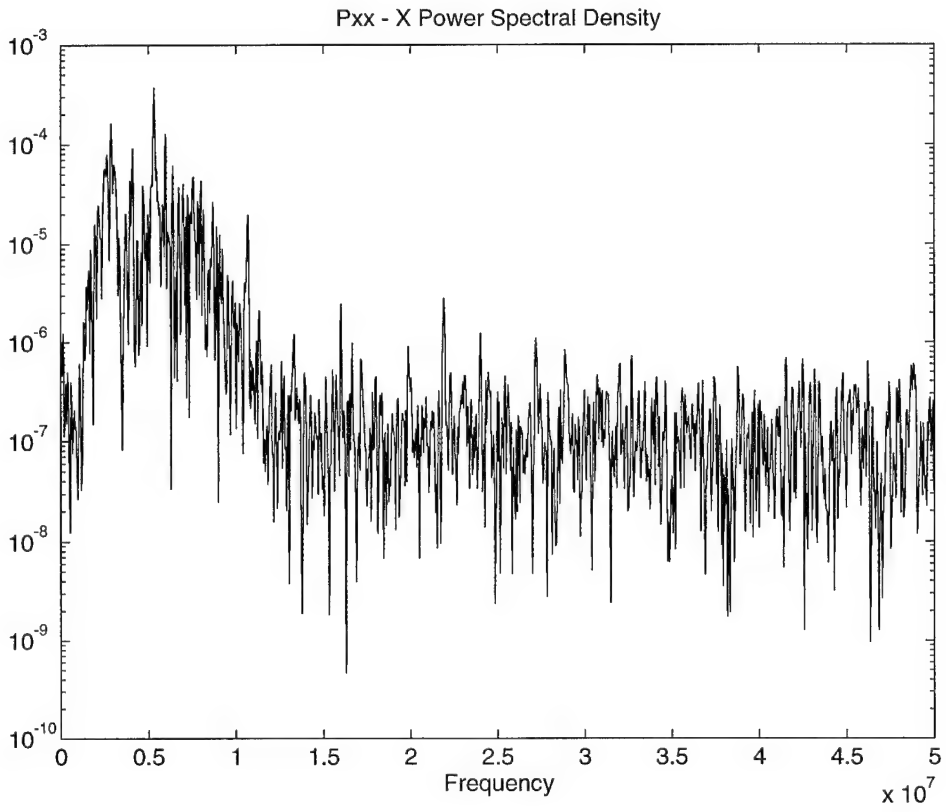

Figure 5: Power spectrum of the A-line data shown in figure 3 obtained using the *spectrum* call in MATLAB.

3 Numerical Methods

Solution of the wave equation can be accomplished through many methods. Choice of the best solution method is dictated by many concerns including the dimension of the problem, extent of the medium, property variation within the medium and knowledge of the boundary conditions. When modeling ultrasound transmission through the diseased breast, especially a post-mastectomy breast, it will be important to use a solution method that will accurately track the reflections, refractions, and attenuation of the sound field.

The acoustical wave equation, for variable properties and attenuation, in the frequency domain is derived in Appendix A. The derivation is presented here so that all the approximations and working assumptions are clearly identified.

3.1 Green's Function

One of the earliest methods used to solve for the pressure field from a transducer was a Green's function like solution for a homogeneous semi-infinite medium [48]. This solution method has been applied to spherical focused transducers [19, 49], and rectangular planar transducers [50] in homogeneous semi-infinite tissue medium. This method models the transducer face as a distribution of point sources. The field for each point source is determined from the free space Green's function solution of equation 19 with homogeneous properties in an infinite medium. Then the pressure field at any point in space is found by summing up the pressures from this distribution of point sources on the transducer. It is customary to work with the velocity potential [21], Ψ, for which the summation has the form,

$$\Psi(r) = \frac{1}{2\pi} \int \int_s v_s \frac{e^{ikr}}{r} ds \tag{6}$$

The pressure is then given by

$$p(r) = \rho \frac{\partial \Psi}{\partial t} = ikZ\Psi \tag{7}$$

This solution is valid for semi-infinite homogeneous regions with constant properties. Attenuation has been included in the previous models by multiplying the pressure by $e^{-\alpha z}$ where z is the depth into the attenuating medium and α is the attenuation coefficient [21]. This method has been extended to regions with variable properties in layered arrangement [51, 52]. Finally, some researchers have expressed the resulting power distribution by curve fitting a two-dimensional Gaussian equation to the solutions obtained by the previous methods [53, 54].

Experimental verification of these models has been done *in vivo* [55] and on non-tissue platforms [56].

3.2 Finite Element Method

The solution of acoustic wave equation 24 can also be achieved by directly solving the governing partial differential equation through application of appropriate numerical techniques such as the

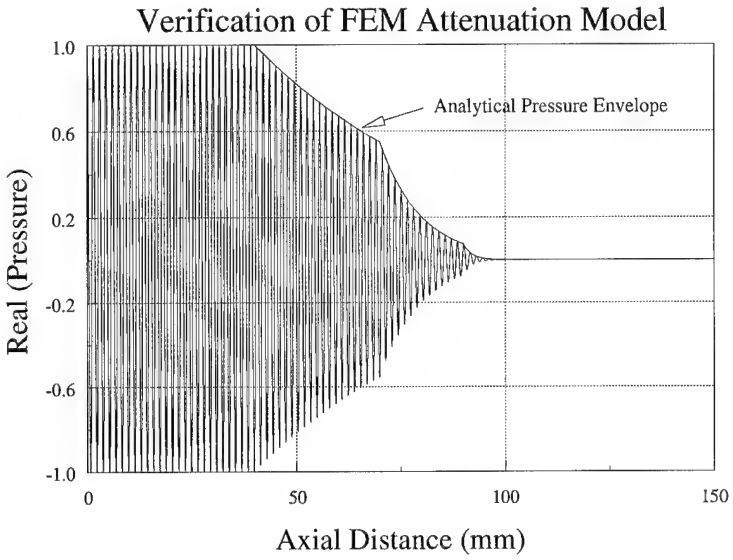

Figure 6: One dimensional verification run on the two dimensional finite elements code to verify the accuracy of the code to model attenuation through the use of a complex wave number.

finite element method. The solution can be developed utilizing any standard finite element method (for example, the Galerkin Method) since the wave equation is self-adjoint [57, 58]. The complex wave equation does possess one additional complexity not mentioned in the usual finite elements texts — the variables are complex numbers. This can be readily handled by most FORTRAN finite elements codes by simply making the variables complex since the FORTRAN language has the built in ability to handle complex numbers [59].

A two dimensional finite elements code has been written to solve equation 24. Verification runs are currently underway. As an example figure 6 shows a verification run of a one dimensional problem to verify the ability of the code to model attenuation through the use of a complex wave number.

3.3 Inverse Techniques

Inverse problems arise when the physical environment either severely limits or completely prohibits the direct measurement of the parameters necessary to uniquely determine a system's dependent variables. When using ultrasound hyperthermia to treat breast cancer the parameters of interest are the spatial distribution and values of: 1) tissue acoustical absorption, 2) attenuation, and 3)

acoustic impedance. The variable of interest is the absorbed power. If one knows all the parameters of a problem then it is possible to solve the "forward" problem for the dependent variables using the differential wave equation, equation 24. The inverse problem arises when one does not know the parameters but is able to measure some other property of the system, usually one of the variables. For ultrasound hyperthermia of breast cancer it is possible to pre-determine geometric regions of constant property (see section 2.1.1) and then measure on-line the value of the absorbed power (see section 2.2.2) at a limited number of internal points — the thermocouple junctions.

The inverse technique developed for this research utilizes a standard inverse technique for non-linear problems [60] that is based on minimizing the error between the model estimated absorbed powers and the clinically measured absorbed powers. The minimization is accomplished by changing the value of the unknown parameters in the model until the "cost" function,

$$\Phi(e) = \sum_{i=1}^{Nm} e_i^2 \quad e_i = Q_i^{\text{measured}} - Q_i^{\text{modeled}} \tag{8}$$

is minimized. This technique is also termed *parameter estimation.* The inverse process begins by assuming some value for the unknown parameters and solving the "forward" problem. The error between the model estimated dependent variables, or parameters, and the measured dependent variables and the resulting changes in absorbed power are given by the following linear approximation:

$$[J](\Delta\gamma) = (e) \tag{9}$$

The "Jacobian" matrix, J, is constructed from numerical simulations and is given by

$$\mathbf{J} = \begin{bmatrix} \frac{\partial Q_1}{\partial \gamma_1} & \frac{\partial Q_1}{\partial \gamma_2} & \cdots & \frac{\partial Q_1}{\partial \gamma_{Np}} \\ \frac{\partial Q_2}{\partial \gamma_1} & \frac{\partial Q_2}{\partial \gamma_2} & \cdots & \frac{\partial Q_2}{\partial \gamma_{Np}} \\ \vdots & \vdots & \ddots & \vdots \\ \frac{\partial Q_{Nm}}{\partial \gamma_1} & \frac{\partial Q_{Nm}}{\partial \gamma_2} & \cdots & \frac{\partial Q_{Nm}}{\partial \gamma_{Np}} \end{bmatrix} \tag{10}$$

The inverse method utilized herein follows the following cycle of calculations in which the model parameters, γ, are updated according to equation 9 until there is negligible changes.

1. Using the current values of model parameters, γ, calculate the Jacobian in equation 10
2. Construct the error vector using the current values of model parameters, γ
3. Invert equation 9 using singular value decomposition (SVD) to solve for changes in model parameters, γ
4. Update model parameters
5. Stop if the change in model parameters is small or the error, e, is acceptable

4 Conclusions

The equipment and techniques necessary to perform the RF and temperture data acquisition needed for the inverse technique has been purchased and or fabricated. Two state of the art numerical solution techniques have been developed to solve for the pressure field in inhomogeneous tissue.

5 Future Work

5.1 Experimental Methods

Evaluation of the various methods to estimate the tissue attenuation coefficient from the digitized RF data needs to be completed. This includes numerical simulations to determine the theoretical influence of noise, sampling rate, and digital signal processing techniques. For example, which power spectrum estimation technique provides the most accuracy. Additionally the effect of time gain compensation, dynamic focusing, and diffration need to be compensated for.

The errors in using a clinical thermocouple probe to measure the absorbed power need to be quantified. If required, limited design modifications can be made to the clinical probe to improve the measurement accuracy.

5.2 Numerical Methods

The finite element and layered Green's function approach [52] need to be compared to determine relative accuracy and speed. The forward solver is at the heart of the inverse technique, and choise of the optimal forward solution algorithm is therefore essential.

5.2.1 Combined Solution Algorithm

The two solution algorithms (integral equation and differential equation) discussed above each possess positive and negative attributes when solving for any given problem. It is possible to optimally combine them in a hybrid solution method that utilizes the positive aspects of each method. The solution method to be developed herein will utilize the following scheme:

1. Use the superposition method to propagate the sound field *from* the transducer surface *to* the tissue interface. Since the sound propagates from the transducer through a homogeneous medium it makes sense to use the simplest, fastest method for this region. This method then provides the complex pressures at the tissue boundary.

2. Use the complex pressures from the superposition method as boundary conditions for the finite elements solution of equation 24.

This solution method has the following additional (beyond those inherit in the finite elements solution and the superposition solution) assumptions:

1. There is no sound reflection or refraction at the water–tissue interface.

2. Boundary conditions for the other tissue surfaces must be assumed–usually taken as zero.

5.3 Inverse Techniques

Since the unknown model parameters, γ, will have different units, equation 8 can be modified to normalize, or nondimensionalize, the error quantities. This may improve the stability of the inverse technique. It may also be possible to introduce some form of regularization when inverting equation 9.

References

[1] Anonymous. Diagnostic and therapeutic technology assessment. hyperthermia as adjuvant treatment for recurrent breast cancer and primary malignant glioma. *Journal of the American Medical Association*, 271:797–802, 1994.

[2] B.A. Bornstein, P.S. Zouranjian, J.L. Hansen, S.M. Fraser, L.A. Gelwan, B.A. Teicher, and G.K. Svensson. Local hyperthermia, radiation therapy, and chemotherapy in patients with local-regional recurrence of breast carcinoma. *International Journal of Radiation Oncology Biology Physics*, 25:79–85, 1993.

[3] J. Overgaard, D.G. Gonzalez, M.C.C.M. Hulshof, G. Arcangeli, O. Dahl, O. Mella, and S.M. Bentzen. Randomized trial of hyperthermia as adjuvant to radiotherapy for recurrent or metastatic malignant melanoma. *Lancet*, 345:540–543, 1995.

[4] M. Amichetti, R. Valdagni, C. Graiff, and A. Valentini. Local-regional recurrences of breast cancer: Treatment with radiation therapy and local microwave hyperthermia. *American Journal of Clinical Oncology*, 14:60–65, 1991.

[5] J.B. DuBois, M. Hay, and G. Bordure. Superficial microwave-induced hyperthermia in the treatment of chest wall recurrences in breast cancer. *Cancer*, 66:848–852, 1990.

[6] K. Hynynen, R.B. Roemer, D.P. Anhalt, C.J. Johnson, Z. Zu, W. Swindell, and T.C. Cetas. A scanned focused, multiple transducer ultrasonic system for localized hyperthermia treatments. *International Journal of Hyperthermia*, 3(1):21–35, 1987.

[7] J.R. Oleson. Adjuvant hyperthermia for recurrent breast cancer. *International Journal of Radiation Oncology Biology Physics*, 24:381–382, 1992.

[8] J.R. Oleson, T.V. Samulski, K.A. Leopold, S.T. Clegg, M.W. Dewhirst, R.K. Dodge, and S.K. George. Sensitivity of hyperthermia trail outcomes to temperature and time: Implications for thermal goals of treatment. *International Journal of Radiation Oncology Biology Physics*, 25:289–297, 1993.

[9] P.M. Harari, K.H. Hynynen, R.B. Roemer, D.P. Anhalt, D.S. Shimm, B. Stea, and J.R. Cassady. Development of scanned focussed ultrasound hyperthermia: Clinical response evaluation. *International Journal of Radiation Oncology Biology Physics*, 21:831–840, 1991.

[10] D.M. Sullivan, R. Ben-Yosef, and D.S. Kapp. Stanford 3d hyperthermia treatment planning system. technical review and clinical summary. *International Journal of Hyperthermia*, 9(5):627–643, 1993.

[11] E.J. Halpern. Calculation of tissue attenuation with a clinical ultrasound unit. *Investigative Radiology*, 28:598–603, 1993.

[12] B.S. Garra, T.H. Shawker, M. Nassi, and M.A. Russel. Ultrasound attenuation measurements of the liver in vivo using a commercial sector scanner. *Ultrasonic Imaging*, 6:396–407, 1984.

[13] A. Shmulewitz, Z. Heyman, E. Walach, B. Ramot, and Y. Itzchak. Ultrasonic attenuation maps of liver based on conventional b-scan and an amplitude loss technique. *Investigative Radiology*, 25:1095–1101, 1990.

[14] K. Itoh, Y. Yasuda, O. Suzuki, H. Itoh, T. Itoh, T. Jing-Wen, T. Konishi, and A. Koyano. Studies on frequency-dependent attenuation in the normal liver and spleen and in the liver diseases, using spectral-shift zero-crossing method. *Journal of Clinical Ultrasound*, 16:553–562, 1988.

[15] F.T. D'Astous and F.S. Foster. Frequency dependence of ultrasound attenuatin and backscatter in breast tissue. *Ultrasound in Medicine and Biology*, 12(10):795–808, 1986.

[16] G. Berger, P. Laugier, J.C. Thalabard, and J. Perrin. Global breast attenuation: Control group and benign breast diseases. *Ultrasonic Imaging*, 12:47–57, 1990.

[17] R. Kuc and K.J.W. Taylor. Variation of acoustic attenuation coefficient slope estimates for Iin IVivo liver. *Ultrasound in Medicine and Biology*, 8(4):403–412, 1982.

[18] K.J. Parker, M.S. Asztely, R.M. Lerner, E.A. Schenk, and R.C. Waag. IIn-Vivo measurements of ultrasound attenuation in normal or diseased liver. *Ultrasound in Medicine and Biology*, 14(2):127–136, 1988.

[19] H.T. O'Neil. Theory of focusing radiators. *Journal of the Acoustical Society of America*, 21(5):516–526, 1949.

[20] A.B. Bhatia. *Ultrasonic Absorption.* Dover (orig. Oxford University Press, Inc. 1967), New York, 1st edition, 1985.

[21] A.D. Pierce. *Acoustics An Introduction to Its Physical Principles and Applications.* Acoustical Society of America, Woodbury, New York, 2nd edition, 1989.

[22] P.M. Morse and K.U. Ingar. *Theoretical Acoustics.* Princeton University Press, Princeton, NJ, 1968.

[23] J. Ophir, T.H. Shawker, N.F. Maklad, J.G. Miller, S.W. Flax, P.A. Narayana, and J.P. Jones. Attenuation estimation in reflection: Progress and prospects. *Ultrasonic Imaging*, 6:349–395, 1984.

[24] K.K. Shung and G.A. Thieme. *Ultrasonic Scattering in Biological Tissues.* CRC Press, Boca Ratan, Florida, 1993.

[25] R. Kuc and M. Schwartz. Estimating the acoustic attenuation coefficient slope for liver from reflected ultrasound signals. *IEEE Transactions on Sonics and Ultrasonics*, SU-26:353–362, 1979.

[26] L.S. Wilson, M.L. Neale, H.E. Talhami, and M. Appleberg. Preliminary results from attenuation-slope mapping of plaque using intravascular ultrasound. *Ultrasound in Medicine and Biology*, 20(6):529–542, 1994.

[27] B.S. Garra, M.F. Insana, T.H. Shawker, and M.A. Russell. Quantitative estimation of liver attenuation and echogenicity: Normal state versus diffuse liver disease. *Radiology*, 162:61–67, 1987.

[28] L.S. Wilson, D.E. Robinson, and B.D. Doust. Frequency domain processing for ultrasonic attenuation measurement in liver. *Ultrasonic Imaging*, 6:278–292, 1984.

[29] M. O'Donnell. Effects of diffraction on measurements of the frequency-dependent ultrasonic attenuation. *IEEE Transactions on Biomedical Engineering*, BME-30:320–325, 1983.

[30] I. Cespedes and J. Ophir. Diffraction correction methods for pulse-echo acoustic attenuation estimation. *Ultrasound in Medicine and Biology*, 16(7):707–717, 1990.

[31] I. Cespedes and J. Ophir. Correction of diffraction errors in attenuation estimation with dynamic beam translation. *Ultrasound in Medicine and Biology*, 18(2):213–218, 1992.

[32] S.W. Flax, J.P. Norbert, G.H. Glover, F.D. Gutmann, and M. McLachlan. Spectral characterization and attenuation measurements in ultrasound. *Ultrasonic Imaging*, 5:95–116, 1983.

[33] Bao-W. Dong, M. Wnag, Ke Xie, and Min-H. Chen. In vivo measurements of frequency-dependent attenuation in tumors of the liver. *Journal of Clinical Ultrasound*, 22:167–174, 1994.

[34] J. Ophir, M.A. Ghouse, and L.A. Ferrari. Attenuation estimation with the zero-crossing technique: Phantom studies. *Ultrasonic Imaging*, 7:122–132, 1985.

[35] E. Walach, A. Shmulewitz, Y. Itzchak, and Z. Heyman. Local tissue attenuation images based on pulsed-echo ultrasound scans. *IEEE Transactions on Biomedical Engineering*, 36:211–221, 1989.

[36] E. Walach, C.N. Liu, R.C. Waag, and K.J. Parker. Quantitative tissue characterization based on pulsed-echo ultrasound scans. *IEEE Transactions on Biomedical Engineering*, BME-33:637–643, 1986.

[37] M. Fink, F. Hottier, and J.F. Cardoso. Ultrasonic signal processing for in vivo attenuation measurement: Short time fourier analysis. *Ultrasonic Imaging*, 5:117–135, 1983.

[38] C.R. Meyer. An iterative, parametric spectral estimation technique for high- resolution pulse-echo ultrasound. *IEEE Transactions on Biomedical Engineering*, BME-26:207–212, 1979.

[39] K. Zhou, D. Zhang, C. Lin, and S. Zhu. Ultrasonic attenuation estimation in-vivo using the difference ratio correction method. *Journal of the Acoustical Society of America*, 92(5):2532–2538, 1992.

[40] F.W. Kremkau. *IEEE Guide for Medical Ultrasonic Field Parameter Measurements - Std 790-1989.* The Institute of Electical and Electronics Engineers, Inc., New York, 1st edition, 1989.

[41] W.J. Fry and R.B. Fry. Determination of absolute sound levels an acoustic absorption coefficients by thermocouple probes - experiment. *Journal of the Acoustical Society of America*, 26(3):311–317, 1954.

[42] W.J. Fry and R.B. Fry. Determination of absolute sound levels and acoustic absorption coefficients by thermocouple probes - theory. *Journal of the Acoustical Society of America*, 26(3):294–310, 1954.

[43] C.J. Martin and A.N.R. Law. The use of thermistor probes to measure energy distribution in ultrasound fields. *Ultrasonics*, 18:127–133, 1980.

[44] C.J. Martin, K. Hynynen, and D.J. Watmough. Measurement of ultrasound energy density distributions in vivo. *Ultrasound in Medicine and Biology*, 10(6):701–708, 1984.

[45] K.J. Parker. The thermal pulse decay technique for measuring ultrasonic absorption coefficients. *Journal of the Acoustical Society of America*, 74(5):1356–1361, 1983.

[46] A.A.C. De Leeuw, J. Crezee, and J.J.W. Lagendijk. Temperature and sar measurements in deep-body hyperthermia with thermocouple thermometry. *International Journal of Hyperthermia*, 9(5):685–697, 1993.

[47] W.L. Nyborg. Heat generation by ultrasound in a relaxing medium. *Journal of the Acoustical Society of America*, 70(2):310–312, 1981.

[48] H. Lamb. *Hydrodynamics.* Cambridge University Press, New York, 6th edition, 1932.

[49] W.G.R. Gibson and R.S.C. Cobbold. Ultrasonic fields of a convex semispherical transducer. *Journal of the Acoustical Society of America*, 94(4):1923–1929, 1993.

[50] K. Ocheltree and L. Frizzell. Sound field calculation for rectangular sources. *IEEE Transactions on Ultrasonics, Ferroelectronics, and Frequency Control*, 36:242–248, 1989.

[51] X. Fan and K. Hynynen. The effects of curved tissue layers on the power deposition patterns of therapeutic ultrasound beams. *Medical Physics*, 21:25–34, 1994.

[52] J.W. Wiskin. *Geometric and Integral Equation Methods in Scattering in Layered Media.* PhD thesis, University of Utah, Salt Lake City, 1991.

[53] J. Wu and D. Gonghuan. Temperature elevation generated by a focused gaussian beam of ultrasound. *Ultrasound in Medicine and Biology*, 16(5):489–498, 1990.

[54] J. Wu and W.L. Nyborg. Temperature rise generated by a focussed gaussian beam in a two-layer medium. *Ultrasound in Medicine and Biology*, 18(3):293–302, 1992.

[55] E.G. Moros and K. Hynynen. A comparison of theoretical and experimental ultrasound field distributions in canine muscle tissue in vivo. *Ultrasound in Medicine and Biology*, 18(1):81–95, 1992.

[56] X. Fan and K. Hynynen. The effect of wave reflection and refraction at soft tissue interfaces during ultrasound hyperthermia treatments. *Journal of the Acoustical Society of America*, 91(3):1727–1736, 1992.

[57] D.W. Pepper and J.C. Heinrich. *The Finite Method: Basic Concepts and Applications.* Hemisphere Publishing Corporation, Washington, 1st edition, 1992.

[58] H. Gan, P.L. Levin, and R. Ludwig. Finite element formulation of acoustic scattering phenomena with absorbing boundary condition in the frequency domain. *Journal of the Acoustical Society of America*, 94(3):1651–1662, 1993.

[59] D.R. Lynch, K.D. Paulsen, and J.W. Strohbehn. Finite element solution of maxwell's equations for hyperthermia treatment planning. *Journal of Computational Physics*, 58:246–269, 1985.

[60] Y. Bard. *Nonlinear Parameter Estimation.* Academic Press, Inc., New York, 1974.

A Derivation of the Wave Equation

The acoustic wave equation is derived from the equations of motion for a fluid as illustrated in figure 7. The first equation is *conservation of mass*, which states that the rate of change of density at a point is equal to the net mass flux from that point,

$$\frac{\partial}{\partial t}\rho(\mathbf{x},t) + \nabla \cdot (\rho(\mathbf{x},t)\mathbf{u}) = 0 \tag{11}$$

The second equation is *conservation of momentum*, which states that the net force on a particle is equal the mass of the particle times its acceleration,

$$\rho\frac{D}{Dt}\mathbf{u} + \nabla p = 0 \tag{12}$$

Third we introduce the concept of *linear acoustics.* Simply stated this means that the disturbance produced by the sound wave to the ambient state is "small", and the total field can be considered as the ambient field plus a perturbation.

$$p = p_o + p' \ , \ \rho = \rho_o + \rho' \ , \ \mathbf{u} = \mathbf{u}_o + \mathbf{u}' \tag{13}$$

Forth we introduce a *thermodynamic relationship* between pressure and density that is valid for the cycle produced by the passing of the thermodynamic wave. This can be either an isentropic relationship or an isothermal one. For example in a liquid, this relationship is

$$\kappa_s = \rho_o \left.\frac{\partial p}{\partial \rho}\right|_s \tag{14}$$

Now we can use all the above relations to form the wave equation. First put the linear approximations in equations 11 and 12. Expand these equations out and recall that the ambient field solves the conservation of mass equation and conservation of momentum equation equations exactly in a trivial sense since the ambient field is static. Then introduce equation 14 in what is left of the conservation of mass equation and equations 11 and 12 become,

$$\kappa_s(\mathbf{x})\frac{\partial}{\partial t}\rho'(\mathbf{x},t) + \nabla \cdot \mathbf{u}'(\mathbf{x},t) = 0 \tag{15}$$

$$\rho_o(\mathbf{x})\frac{\partial}{\partial t}\mathbf{u}'(\mathbf{x},t) + \nabla p'(\mathbf{x},t) = 0 \tag{16}$$

In the discussion that follows, only the *acoustic* values of these variables remain (save for ρ_o) and so for convenience sake the $'$ (prime) notation is dropped with the understanding that all variables are the acoustic values. The above two equations can be combined into one equation to form the wave equation which has the form,

$$\kappa_s(\mathbf{x})\frac{\partial^2}{\partial t^2}p(\mathbf{x},t) - \nabla \cdot \left(\frac{1}{\rho_o(\mathbf{x})}\nabla p(\mathbf{x},t)\right) = 0 \tag{17}$$

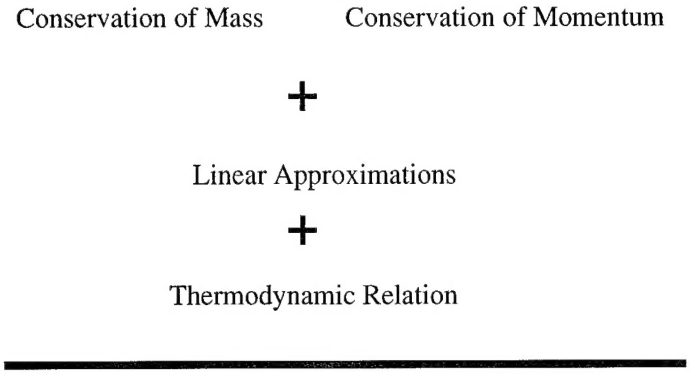

Figure 7: Diagram of the Derivation Process

Now a useful trick here is to Laplace transform equation 17 to remove the time derivative. We will not directly transform equation 17 but instead assume the pressure time relationship given by

$$p = \tilde{A}(\mathbf{x})e^{-i\omega t} \tag{18}$$

where $\tilde{A}(\mathbf{x})$ is a complex pressure amplitude. One way to think about this transformation is that at each point x in the domain the pressure is oscillating at ω radians/sec with an amplitude of $\tilde{A}(\mathbf{x})$. Furthermore since $\tilde{A}(\mathbf{x})$ is a complex number this means that the oscillations may be out of phase with each other. Equation 17 now becomes

$$-\omega^2 \kappa_s(\mathbf{x}) \frac{\partial^2}{\partial t^2} \tilde{p}(\mathbf{x}) - \nabla \cdot \left(\frac{1}{\rho_o(\mathbf{x})} \nabla \tilde{p}(\mathbf{x}) \right) = 0$$

which can be rearranged as

$$\frac{k^2(\mathbf{x})}{\rho(\mathbf{x})} \nabla^2 \tilde{p}(\mathbf{x}) - \nabla \cdot \left(\frac{1}{\rho_o(\mathbf{x})} \nabla \tilde{p}(\mathbf{x}) \right) = 0 \tag{19}$$

where $k = \omega/c$ is the wave number.

We can include the affects of attenuation due to absorption through an analogy to the one dimensional solution. First note that in a one dimensional homogeneous problem the attenuation is taken into account by multiplying the unattenuated pressure value by $exp^{\alpha x}$ (see Pierce for a detailed derivation of this loss), where α is the attenuation coefficient in Nepers meter^{-1} . Recall, or review, that the plane wave solution can be written as

$$\tilde{p}(\mathbf{x}) = \tilde{A}e^{ikx} \tag{20}$$

where $\tilde{A}$ is a complex magnitude that allows for an arbitrary phase offset. Note that the solution for the plane wave equation is accomplished without regard to boundary conditions. To account for attenuation of the wave we simply multiply the pressure by the exponential loss

$$\tilde{p}(\mathbf{x}) = \tilde{A}e^{ikx}e^{-\alpha x} \tag{21}$$

Next we combine the exponentials and define a complex wave number, $\tilde{k}$, given as

$$\tilde{k} = \frac{\omega}{c} + i\alpha \tag{22}$$

Then equation 21 can be written as

$$\tilde{p}(\mathbf{x}) = \tilde{A}e^{i\tilde{k}x} \tag{23}$$

The extension of the complex wave number to account for attenuation loss in three dimensions is straightforward and equation can be written as

$$\frac{\tilde{k}^2(\mathbf{x})}{\rho(\mathbf{x})}\nabla^2\tilde{p}(\mathbf{x}) - \nabla\cdot\left(\frac{1}{\rho_o(\mathbf{x})}\nabla\tilde{p}(\mathbf{x})\right) = 0 \tag{24}$$